

Advanced Ferroelectric $\text{LiNb}_{(1-x)}\text{Ta}_x\text{O}_3$ Crystal: Crystal Growth, Crystal Structure, Physical Properties

D.V. Roshchupkin^{1*}, E.V. Emelin¹, O.A. Plotitsyna¹, R.R. Fahrtdinov¹,
D.V. Irzhak¹, V.K. Karandashev¹, T.V. Orlova¹, B.S. Redkin², H. Fritze³,
Yu. Suhak³

¹ Institute of Microelectronics Technology and High-Purity Materials
of Russian Academy of Sciences

Chernogolovka, 6 Academician Osipyan str., 142432, Moscow District, Russian Federation

² Institute of Solid-State Physics Russian Academy of Sciences,

Chernogolovka, 2 Academician Osipyan str., 142432, Moscow District, Russian Federation

³ Clausthal University of Technology, Institute of Energy Research and Physical Technologies
Leibnizstraße 4, D-38678, Clausthal-Zellerfeld, Germany

*E – mail: rochtch@iptm.ru

Received 23 June 2020

Abstract: The process of promising ferroelectric $\text{LiNb}_{(1-x)}\text{Ta}_x\text{O}_3$ crystals growing by Czochralski method is studied. For the first time $\text{LiNb}_{0.88}\text{Ta}_{0.12}\text{O}_3$ crystals were grown. The composition of the crystals was determined by the method of ion mass spectrometry with inductively coupled plasma. Curie temperature $T_C=1102$ °C was measured by the method of differential scanning calorimetry. The parameters of the crystal unit cell were measured using high-resolution X-ray diffraction. The crystal unit cell parameters a and c occupy an intermediate position between the corresponding values in LiNbO_3 and LiTaO_3 crystals. The use of scanning electron microscopy and high-resolution X-ray diffraction allowed to measure the velocity of surface acoustic waves.

Keywords: crystal growth, crystal structure, LiNbO_3 and LiTaO_3 crystals

1. Introduction

Ferroelectric LiNbO_3 and LiTaO_3 crystals are widely used in acoustoelectronics and acoustooptics due to the high values of the piezoelectric modules. These crystals were first grown by the Czochralski method in the mid-sixties of the last century. Crystals have the same structure and belong to the class of symmetry $3m$, but have a significant difference in melting point and Curie temperatures. So in crystals LiNbO_3 and LiTaO_3 the Curie temperature T_C makes 1190°C and 650°C , and melting temperature T_m makes 1240°C and 1650°C , accordingly.

LiNbO_3 crystal has the higher values of piezoelectric modules, while the LiTaO_3 crystal has the good temperature stability, but lower values of piezoelectric modules. Therefore, in the middle of the 70's there was an idea to grow $\text{LiNb}_{(1-x)}\text{Ta}_x\text{O}_3$ crystals, which would combine the best properties

of LiNbO_3 and LiTaO_3 crystals (high values of piezoelectric modules and good temperature stability). In this direction, a large number of studies have been carried out, but so far attempts to grow $\text{LiNb}_{(1-x)}\text{Ta}_x\text{O}_3$ crystals have been fruitless [1-3]. The growth processes of LiNbO_3 and LiTaO_3 crystals differ only in temperatures in the process of the crystals growth at the same speed of rotation and pulling the crystals out of the melt. The use of the parameters of LiNbO_3 and LiTaO_3 crystal growth process did not allow to grow $\text{LiNb}_{(1-x)}\text{Ta}_x\text{O}_3$ crystals. In [4] it was shown that the use of the conventional Czochralski method does not allow to grow $\text{LiNb}_{(1-x)}\text{Ta}_x\text{O}_3$ crystals because of the wide separation between the solid and liquid phase lines in the phase diagram of the $\text{LiNbO}_3 - \text{LiTaO}_3$ system (Fig. 1).

All attempts to grow $\text{LiNb}_{(1-x)}\text{Ta}_x\text{O}_3$ crystals ended to grow crystals with a large number of pores. It has been demonstrated in [2] that for growing $\text{LiNb}_{(1-x)}\text{Ta}_x\text{O}_3$ crystals by the Czochralski method it is necessary to reduce the rate of pulling the crystal out of the melt. Decrease in crystal speed allowed to grow a small crystal of $\text{LiNb}_{0.9}\text{Ta}_{0.1}\text{O}_3$ composition without pores. The small size of the crystal did not allow to investigate the physical properties of the crystal.

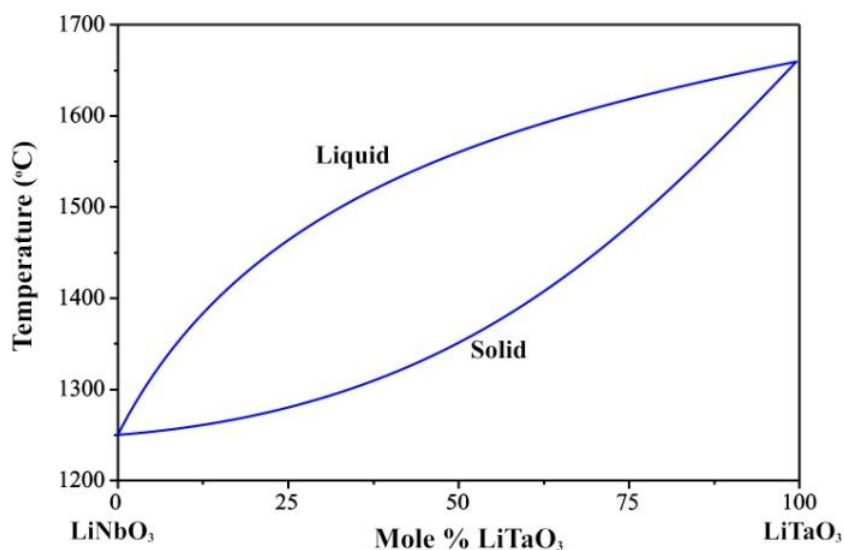


Fig. 1. Phase diagram of the LiNbO_3 - LiTaO_3 system [4].

This paper presents the results on the successful growth of the $\text{LiNb}_{(1-x)}\text{Ta}_x\text{O}_3$ crystals by the Czochralski method and the study of their structural and physical properties.

2. $\text{LiNb}_{(1-x)}\text{Ta}_x\text{O}_3$ crystal growth by Czochralski method

The study of $\text{LiNb}_{(1-x)}\text{Ta}_x\text{O}_3$ crystal growth process by Czochralski method was performed on a NIKA-3M growth machine. For growing $\text{LiNb}_{(1-x)}\text{Ta}_x\text{O}_3$ solid solution the recrystallization method was used, i.e. at the initial stage congruent LiNbO_3 and LiTaO_3 crystals were grown. Then the corresponding proportions of LiNbO_3 and LiTaO_3 crystals were used to grow $\text{LiNb}_{0.88}\text{Ta}_{0.12}\text{O}_3$ crystals. The crystals were grown along axis Z. The use of standard parameters of LiNbO_3 and LiTaO_3 conventional crystal growth process allows to grow crystals with a large number of pores (Fig. 2).



Fig. 2. $\text{LiNb}_{0.88}\text{Ta}_{0.12}\text{O}_3$ crystal grown by conventional Czochralski method.



Fig. 3. $\text{LiNb}_{0.88}\text{Ta}_{0.12}\text{O}_3$ crystal grown by Czochralski method with a very low pulling rate.

Reduction of the crystal pulling rate from the melt by 4 times ($\sim 0.5\text{mm/h}$) allowed to grow crystals with a diameter of 2 cm (Fig. 2). Several crystals of $\text{LiNb}_{0.88}\text{Ta}_{0.12}\text{O}_3$ solid solution were grown, which allowed to carry out a complex study of this material.

3. Investigation of crystal composition, Curie temperature and crystal lattice parameters

Inductively coupled plasma atomic spectrometry was used to study the composition of the grown crystals. This method allowed us to determine the composition of the grown crystal in mass percentages: $\text{Li} - 3.0 \pm 0.1 \text{ mass } \%$, $\text{Nb} - 48.2 \pm 0.5 \text{ mass } \%$, $\text{Ta} - 13.4 \pm 0.2 \text{ mass } \%$. Conversion of mass % into atomic % allowed to determine the composition of the grown crystal: $\text{LiNb}_{0.88}\text{Ta}_{0.12}\text{O}_3$. The composition of the grown crystal was studied at the top, in the middle and at the bottom of the grown crystal and showed the same results.

Differential Scanning Calorimetry has been used to measure the temperature of the Curie, i.e. to determine the temperature of the ferroelectric-paraelectric phase transition. Fig. 4 shows the curve of

heat flow versus heating temperature of the grown crystal $\text{LiNb}_{0.88}\text{Ta}_{0.12}\text{O}_3$. The fracture of the heat flow curve is observed at the temperature of 1102 °C. This fracture corresponds to the Curie temperature $T_C=1102$ °C of these crystals. The measured temperature above Curie temperature of LiTaO_3 crystal, but below Curie temperature of LiNbO_3 crystal.

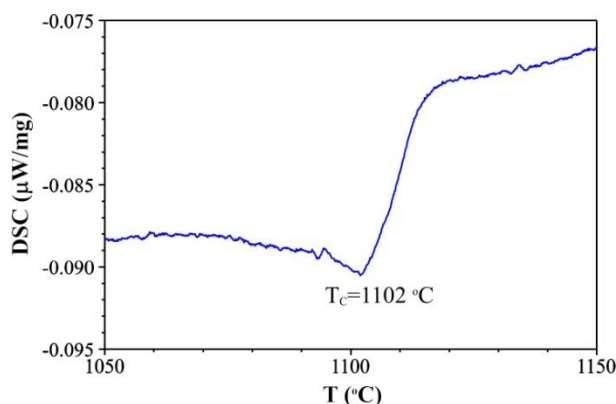


Fig. 4. Change of heat flow versus the crystal heating temperature.

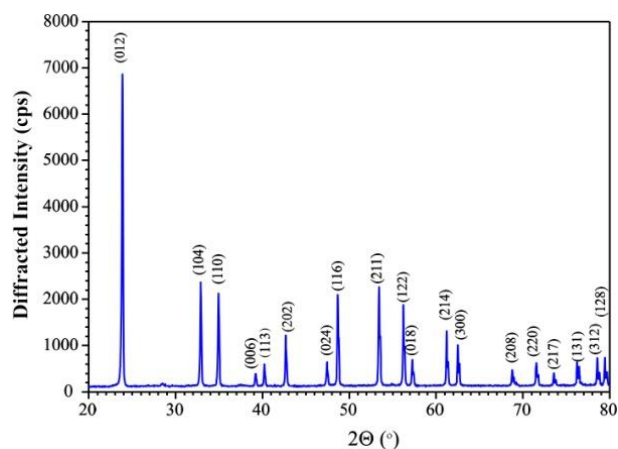


Fig. 5. XRD spectra of a $\text{LiNb}_{0.88}\text{Ta}_{0.12}\text{O}_3$ crystal.

High-resolution X-ray diffraction was used to study the structure of the grown crystal using the 4-circles Bruker D8 DISCOVER X-ray diffractometer. The powder diffraction method in the scheme of a double-crystal X-ray diffractometer was used to measure the XRD spectrum of $\text{LiNb}_{0.88}\text{Ta}_{0.12}\text{O}_3$ crystal (Fig. 5). The elementary crystal unit cell parameters were calculated from measured interplanar spacings. The comparison of parameters of the elementary crystal unit cells in LiNbO_3 , $\text{LiNb}_{0.88}\text{Ta}_{0.12}\text{O}_3$ and LiTaO_3 crystals presents in Table 1. It is seen from Table 1 that parameters of the elementary crystal cells a and c in $\text{LiNb}_{0.88}\text{Ta}_{0.12}\text{O}_3$ crystal occupy an intermediate position between corresponding values in LiNbO_3 and LiTaO_3 crystals.

Table 1. Parameters of the elementary crystal unit cell

N	Crystal	a (Å)	c (Å)
1.	LiNbO_3	5.1502	13.8653
2.	$\text{LiNb}_{0.88}\text{Ta}_{0.12}\text{O}_3$	5.1510	13.8164
3.	LiTaO_3	5.2135	13.7694

4. Acoustic properties of a $\text{LiNb}_{0.88}\text{Ta}_{0.12}\text{O}_3$ crystal

To study the acoustic properties the grown crystal was preliminarily subjected to the monodomenization process, because the ferroelectric domain structure is formed in the process of growth of congruent ferroelectric crystal. During the process of monodomenization, the crystal is heated to Curie temperature, an external electric field is applied to crystal along the polar axis Z , and after crystal is slowly cooled down in the conditions of external electric field application to the crystal. After the monodomenization process, the substrates of the YZ – cut were cut out of the crystal. These substrates are the most used cuts in acoustoelectronics for surface acoustic wave (SAW) devices.

The SAW delay time lines with the structures of interdigital transducer (IDT) were designed on the crystal surface for surface acoustic wave excitation with wavelengths of $\Lambda = 60\mu\text{m}$ and $\Lambda = 4\mu\text{m}$. The process of the SAW excitation and propagation on the crystal surface was studied using different experimental methods. The process of the SAW propagation with wavelength of $\Lambda = 60\mu\text{m}$ was studied using measurement of amplitude-frequency response and scanning electron microscopy.

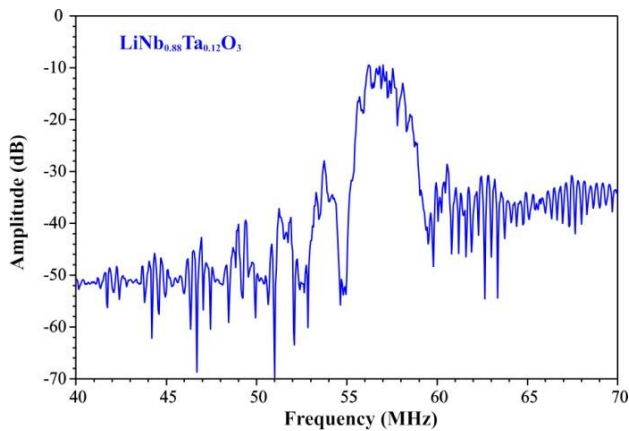


Fig. 6. Amplitude-frequency response of the SAW delay time line with SAW wavelength of $\Lambda=60$

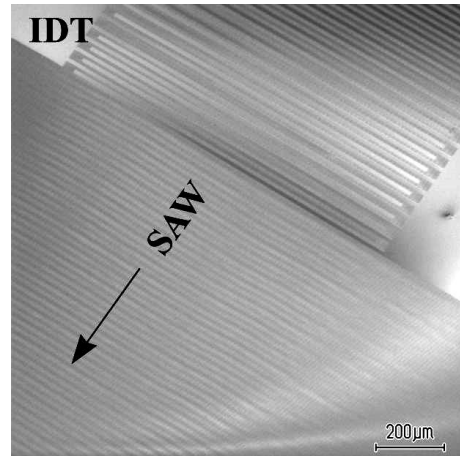


Fig. 7. SEM microphotograph of the SAW propagation in the YZ -cut of a $\text{LiNb}_{0.88}\text{Ta}_{0.12}\text{O}_3$ crystal. $\Lambda=60\mu\text{m}$, $f_0=57.33\text{ MHz}$, $V=3440\text{ m/s}$.

Fig. 6 display the amplitude-frequency response of the delay line based on the YZ – cut of a $\text{LiNb}_{0.88}\text{Ta}_{0.12}\text{O}_3$ crystal. The resonance excitation frequency of the SAW is crystal is

$f_0 = 57.33\text{MHz}$ at the SAW wavelength of $\Lambda = 60\mu\text{m}$, which corresponds to the SAW velocity of $V = \Lambda \times f_0 = 3440\text{m/s}$. The process of the SAW propagation on the surface of the YZ – cut of a $\text{LiNb}_{0.88}\text{Ta}_{0.12}\text{O}_3$ crystal was visualized by scanning electron microscopy method [5]. This method in the low-energy secondary electrons emission mode allows to visualize the acoustic wave fields on the surface of piezoelectric crystals, as the low-energy secondary electrons with energy of $\sim 1\text{eV}$ are sensitive to the electric field that accompanies the SAW propagation in piezo- and ferroelectric crystals. Fig. 7 shows the microphotograph of the SAW with wavelength of $\Lambda = 60\mu\text{m}$ on the surface of the YZ – cut of a $\text{LiNb}_{0.88}\text{Ta}_{0.12}\text{O}_3$ crystal. The SAW propagates along polar axis Z with a velocity of $V = 3440\text{m/s}$.

YZ – cut of a $\text{LiNb}_{0.88}\text{Ta}_{0.12}\text{O}_3$ crystal modulated by SAW with wavelength of $\Lambda = 4\mu\text{m}$ was studied at synchrotron radiation source BESSY II in the scheme of X – ray double axis diffractometer schematically shown in Fig. 8 [6]. The energy of X – ray radiation $E = 10\text{keV}$ was selected by a double $\text{Si}(111)$ – monochromator. X – ray radiation was collimated by primary and secondary slits of 1mm and $50\mu\text{m}$, respectively. X – ray radiation diffracts on an acoustically modulated crystal. SAW propagates in crystal and causes the sinusoidal modulation of the crystal lattice, which acts as a diffraction grating. X – ray radiation diffracts on the acoustically modulated crystal, which leads to the appearance of diffraction satellites on the rocking curve on the both sides of the Bragg peak. The angular divergence between the diffraction satellites is determined by the wavelength of the SAW, and the number of the diffraction satellites and their intensity are determined by the amplitude of the SAW. In the first approximation, the amplitude of the SAW can be determined as $h \sim md / 2\pi$, where m is the number of the diffraction satellites on the rocking curve, d is the interplanar spacing. Diffracted X – ray radiation was recorded by standard scintillation detector NaI.

To study the diffraction process, the reflection from the planes (300) in the acoustically modulated YZ – cut of a $\text{LiNb}_{0.88}\text{Ta}_{0.12}\text{O}_3$ crystal was used. At the SAW wavelength of $\Lambda = 4\mu\text{m}$, the resonant excitation frequency of SAW was $f_0 = 860\text{MHz}$, which corresponds to the SAW velocity of $V = 3440\text{m/s}$. Fig. 9 shows the rocking curve of acoustically modulated crystal, on which a large number of diffraction satellites can be observed. The rocking curve was measured at amplitude of the input high-frequency signal on an IDT of $U = 10\text{V}$. Taking into account the interplanar spacing $d = 1.487\text{Å}$ for reflection (300) and the number of diffraction satellites on the rocking curve $m = 19$, we obtain the value of the SAW amplitude of $h \sim 4.5\text{Å}$.

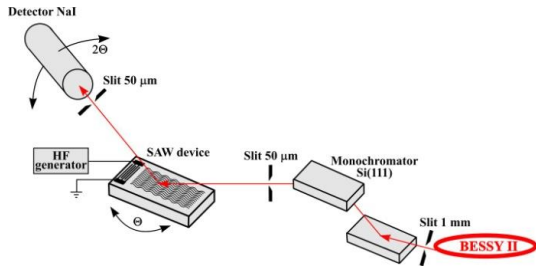


Fig. 8. X-ray double axis diffractometer at synchrotron radiation source BESSY II.

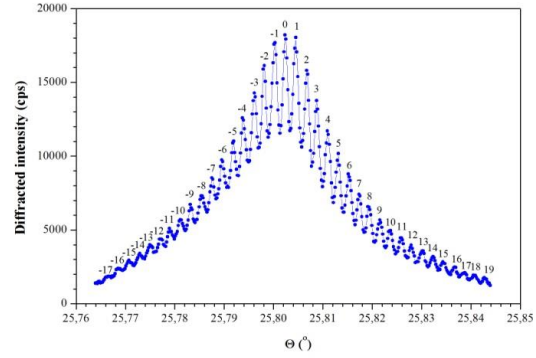


Fig. 9. Rocking curve of a $\text{LiNb}_{0.88}\text{Ta}_{0.12}\text{O}_3$ crystal modulated by SAW with wavelength of $\Lambda=4 \mu\text{m}$. SAW amplitude $h\sim 4.5 \text{ \AA}$, reflection (300).

The investigations by scanning electron microscopy and X-ray diffraction methods allowed to determine the SAW velocity in the YZ – cut of $\text{LiNb}_{0.88}\text{Ta}_{0.12}\text{O}_3$ crystal. Table 2 presents comparison of SAW velocities in LiNbO_3 , $\text{LiNb}_{0.88}\text{Ta}_{0.12}\text{O}_3$ and LiTaO_3 crystals. Table 2 shows that the SAW velocity in the YZ – cut of a $\text{LiNb}_{0.88}\text{Ta}_{0.12}\text{O}_3$ crystal occupies an intermediate position between the corresponding values of the SAW velocity in the LiNbO_3 and LiTaO_3 crystals.

Table 1. SAW velocity in YZ-cut

N	Crystal	V (m/s)
1.	LiNbO_3	3488
2.	$\text{LiNb}_{0.88}\text{Ta}_{0.12}\text{O}_3$	3440
3.	LiTaO_3	3250

5. Conclusion

For the first time the solid solution of ferroelectric $\text{LiNb}_{0.88}\text{Ta}_{0.12}\text{O}_3$ crystals were grown by the Czochralski method. The measured temperature of the ferroelectric phase transition in the crystal was $T_C = 1102^\circ\text{C}$. X – ray powder diffraction method was used to measure the parameters of the elementary crystal unit cell, which were $a = 5.1510 \text{ \AA}$ and $c = 13.8164 \text{ \AA}$. Methods of X – ray high-resolution X – ray diffraction and scanning electron microscopy allowed to determine the SAW velocity in the YZ – cut of $\text{LiNb}_{0.88}\text{Ta}_{0.12}\text{O}_3$ crystal, which was $V = 3440 \text{ m/s}$.

Acknowledgements

The work was done according to the joint project of RFBR (grant #19-52-12044) and DFG (grant # FR1301/32-1).

References

- [1] T. Fukuda, H. Hirano, Solid-solution $\text{LiTa}_x\text{Nb}_{1-x}\text{O}_3$ single crystal growth by Czochralski and edge-defined film-fed growth technique, *J. Crystal Growth*, Vol. 35, 1976, pp. 127-132.
- [2] F. Shimura, Y. Fujino, Crystal growth and fundamental properties of $\text{LiNb}_{1-y}\text{Ta}_y\text{O}_3$, *J. Crystal Growth*, Vol. 38, 1977, pp. 293-302.
- [3] A. Bartasyte, A. M. Glazer, F. Wondre, D. Prabhakaran, P. A. Thomas, S. Huband, D. S. Keeble and S. Margueron, Growth of $\text{LiNb}_{1-x}\text{Ta}_x\text{O}_3$ solid solution crystals, *Mater. Chem. Phys.*, Vol. 134, 2012, pp. 728-735.
- [4] G. E. Peterson, P. M. Bridenbaugh, & P. Green, NMR Study of Ferroelectric LiNbO_3 and LiTaO_3 . I, *J. Chem. Phys.*, Vol. 46, 1967, pp. 4009–4014.
- [5] D. V. Roshchupkin, M. Brunel, Scanning electron microscopy observation of surface acoustic wave propagation in the LiNbO_3 crystals with regular domain structures, *IEEE Transaction on Ultrasonics, Ferroelectrics, and Frequency Control*, Vol. 41, 1994, pp. 512-517.
- [6] R. Tucoulou, F. de Bergevin, O. Mathon, D. Roshchupkin, X-ray Bragg diffraction of LiNbO_3 crystals excited by surface acoustic waves, *Physical Review B*, Vol. 64, 2001, pp. 134108(9).